Published in final edited form as:
Cancer Res. 2008 December 1; 68(23): 9996–10003. doi:10.1158/0008-5472.CAN-08-2492.

Coevolution of Prostate Cancer and Bone Stroma in Three-Dimensional Coculture: Implications for Cancer Growth and Metastasis

Shian-Ying Sung[1,2,10], **Chia-Ling Hsieh**[1,10,11], **Andrew Law**[6], **Haiyen E. Zhau**[1], **Sen Pathak**[5], **Asha S. Multani**[5], **Sharon Lim**[3], **Ilsa M. Coleman**[8], **Li-Chin Wu**[10], **William D. Figg**[9], **William L. Dahut**[9], **Peter Nelson**[8], **Jae K. Lee**[7], **Mahul B. Amin**[3], **Robert Lyles**[4], **Peter A.J. Johnstone**[2], **Fray F. Marshall**[1], and **Leland W.K. Chung**[1]

[1]Department of Urology, Emory University School of Medicine, Atlanta, Georgia [2]Department of Radiation Oncology, Emory University School of Medicine, Atlanta, Georgia [3]Department of Pathology, Emory University School of Medicine, Atlanta, Georgia [4]Department of Biostatistics and Bioinformatics, Emory University Rollin School of Public Health, Atlanta, Georgia [5]Department of Molecular Genetics, The University of Texas M. D. Anderson Cancer Center, Houston, Texas [6]Department of Urology, University of Virginia, Charlottesville, Virginia [7]Department of Public Health Sciences, University of Virginia, Charlottesville, Virginia [8]Fred Hutchinson Cancer Center, Seattle, Washington [9]Center for Cancer Research, National Cancer Institute, Bethesda, Maryland [10]Center for Molecular Medicine and Graduate Institute of Cancer Biology, China Medical University and Hospital, Taichung, Taiwan, ROC [11]Department of Biotechnology, Asia University, Wufeng, Taichung, Taiwan, ROC

Abstract

Human bone stromal cells, after three-dimensional coculture with human prostate cancer (PCa) cells *in vitro*, underwent permanent cytogenetic and gene expression changes with reactive oxygen species serving as mediators. The evolved stromal cells are highly inductive of human PCa growth in mice, and expressed increased levels of extracellular matrix (versican and tenascin) and chemokine (*BDFN*, *CCL5*, *CXCL5*, and *CXCL16*) genes. These genes were validated in clinical tissue and/or serum specimens and could be the predictors for invasive and bone metastatic PCa. These results, combined with our previous observations, support the concept of permanent genetic and behavioral changes of PCa epithelial cells after being either cocultured with prostate or bone stromal cells as three-dimensional prostate organoids or grown as tumor xenografts in mice. These observations collectively suggest coevolution of cancer and stromal cells occurred under three-dimensional growth condition, which ultimately accelerates cancer growth and metastasis.

Introduction

Tumor-microenvironment interactions are crucial in oncogenesis and cancer progression. Genetic studies using laser captured microdissection and gene expression profiling of

Requests for reprints: Leland W. K. Chung, Molecular Urology and Therapeutics Program, Department of Urology, Emory University School of Medicine, 1365B Clifton Road, Room B5101, Atlanta, GA 30322. Phone: 404-778-3672; Fax: 404-778-778-3965; lwchung@emory.edu.

Note: Supplementary data for this article are available at Cancer Research Online (http://cancerres.aacrjournals.org/).

Disclosure of Potential Conflicts of Interest
No potential conflicts of interest were disclosed.

clinical specimens confirmed genetic and gene expression changes in tumor cells (1) and adjacent stroma (2). Although genetic and gene expression changes in cancer cells are expected, similar changes in the stroma in response to cancer epithelium and their potential functions are less well-defined. Pathak and colleagues (3) showed mouse stromal fibroblasts harvested from human prostate cancer (PCa) xenografts exhibited identical and nonrandom genetic changes. Coculture of human prostate or bone stromal cells with human PCa LNCaP (LN) cells under three-dimensional conditions induced permanent genetic, morphologic, and behavioral changes in LN cells (4). Hill and colleagues (5) showed that conditional disruption of an epithelial cell-specific pRB function in the mouse prostate epithelium induced permanent p53 genetic changes in the tumor-adjacent stroma. Bhowmick and colleagues (6) showed that transgenic mice with transforming growth factor (TGF)β signaling interrupted by conditional inactivation of the TGFβ type II receptor gene in mouse prostate and fore-stomach stromal fibroblasts developed intraepithelial neoplasia in the prostate and invasive squamous cell carcinoma in the fore-stomach, possibly by activation of paracrine hepatocyte growth factor signaling. Because spontaneously immortalized stromal fibroblasts (7) or fetal urogenital sinus mesenchymes (8) are highly inductive, promoting the growth and progression of prostate tumors in mice and that permanent gene expression and behavior changes were observed in epithelial cells upon cellular interaction with stroma (9–11), we focused here on defining if prostate stromal fibroblasts “coevolve” with cancer epithelial cells through reciprocal cancer-stroma interaction and the altered stromal fibroblasts may be responsible for enhancing tumor progression through enhanced paracrine signaling.

Tumor growth in the primary or metastatic site is constantly modulated by stress conditions, including fluctuations in nutrition, pH, hypoxia, osmotic, and hormonal conditions (12, 13). Reactive oxygen species (ROS) are common mediators of stress and inflammatory responses, implicated in cancer progression by causing DNA damage and inducing genomic instability in cancer epithelium and stroma fibroblasts (14, 15). In this communication, we showed marked cytogenetic, gene expression and behavioral changes in bone cells cocultured under three-dimensional conditions with PCa cells, with ROS serving as the critical mediators. The genetically altered bone stromal cells are highly inductive of human PCa growth and progression. Gene expression profiling of altered bone stromal cells revealed unique molecular signatures shared with cancer-associated prostate stromal fibroblasts, confirmed in clinical PCa tissue and serum specimens from patients with progressive PCa.

Materials and Methods

Cell lines and culture

LN and its lineage-derived C4-2 and C4-2B human PCa epithelial cell lines were obtained from *in vivo* cellular interaction between LN and a human bone stromal MS cell line (10). MG-63, a human osteosarcoma cell line, HS27A, an immortalized human osteoblast, and HFOB, a human fetal osteoblast (American Type Culture Collection), were cultured in T-medium (Invitrogen) with 5% fetal bovine serum (FBS; Sigma) at 37°C. Human prostate fibroblasts from normal/benign and cancerous areas of prostatectomy specimens were confirmed by positive vimentin but negative desmin and cytokeratin IHC staining.

Three-dimensional coculture of PCa and bone stromal cells in RWV

LN, C4-2, MG-63, HFOB, and HS27A cells were seeded in T-medium with 10% FBS, switched to 5% FBS, and maintained within 20 passages. LN and C4-2 cells were recovered from a cryopreserved stock (passage between 15 and 20) 2 wk before the experiment. MG-63, HFOB, or HS27A cells (passage number between 5 and 10) were recovered

similarly 1 wk before the experiment. Coculture was done in three-dimensional RWV conditions with or without microcarrier beads according to previously published methods (4). We noted no morphologic and gene expression differences in cells harvested from cocultured PCa and bone stromal cells either with or without microcarrier beads. A culture medium sample was collected every 3 d for monitoring prostate-specific antigen (PSA) and replaced with 30 mL fresh medium. Cocultured organoids were harvested after 2 or 3 wk with dispase (5 mg/mL; Roche) or trypsin (0.25% v/v; Invitrogen). Cells grown from prostate organoids were separated by differential attachment to the plastic dish (4, 10).

Freshly harvested and pathologically confirmed cancer tissue specimens were obtained from the peripheral zone of the prostate gland with the contralateral normal/benign prostate tissues serve as controls. Tissues were minced to <1 mm^3, adhered to plastic culture dishes, and cultured under sterile conditions with T-Medium and 10% FCS (10). Epithelial cells were removed by trypsin and EDTA followed by mechanical irrigation with tissue culture medium. Pure prostate stromal fibroblasts, by morphologic and immunohistochemical (IHC) criteria (vimentin positive and cytokeratin and desmin negative), were obtained after 8 to 12 rounds of subculture. PCa epithelial and prostate or bone stromal cells were confirmed by cell morphology, IHC staining, and PSA production. In this study, we have isolated paired stromal fibroblasts from normal/benign and cancerous areas of tissue specimens from five patients, designated respectively as Pt1-N to Pt5-N and Pt1-C to Pt5-C. The clonal nature of the harvested cells was cytogenetically established by conventional Giemsa (G) banding analysis using previously published methods (16).

Animal study

Six-week-old athymic nude mice [BALB/c; National Cancer Institute (NCI)] were used. Animal protocols were approved by the Emory IACUC Committee. To produce chimeric tumors, 2×10^6 cells per 100 μL per site were injected s.c. with a 4:1 ratio of mixed C4-2-Luc (C4-2 cells stably transfected with a luciferase expression vector) and parental MG63 or its lineage-derived cells using a previously established coinoculation method (17). Tumor volume, serum PSA level, and tumor-associated luciferase activity were determined by established protocols (10, 17, 18).

Immunohistochemistry

Five-micrometer paraffin-embedded tissue sections were deparaffinized and rehydrated, antigens were retrieved, and IHC procedures were performed using published methods (10, 17). The antibodies are as follows: mouse monoclonal anti-human tenascin (1:50 dilution; Chemicon International, Inc.), mouse monoclonal anti-versican (1: 50 dilution; provided by Dr. Richard Asher, Cambridge UK), mouse monoclonal anti-human osteonectin (0.1 ug/mL; Haematologic Technologies, Inc.), or mouse monoclonal anti–brain-derived neutrophic factor (BDNF; 2.5 ug/mL; R&D Systems). Specificity of the immunostaining was determined by the inclusion of isotype-specific IgG as negative controls and normal human skin epidermis for tenascin, dermis for versican, and nerve trunk tissue for osteonectin as positive controls.

Quantitative reverse transcription-PCR

Quantitative reverse transcription PCR (qRT-PCR) was performed using the iCycler thermal cycler system (Bio-Rad) according to the manufacturer's instructions. In brief, 5 μg RNA isolated from cells at 80% to 95% confluency, following the protocol from Qiagen, were used for reverse transcription reaction using the Moloney murine leukemia virus RT system (Invitrogen) and random primer. Quantitative PCR was performed by the LightCycler 480 system (Roche Applied Science) using a 2× PCR Master mix (Roche Applied Science) and Universal Probe Library (Roche Applied Science). To determine gene expression levels

between specimens, $2^{-\Delta\Delta Ct}$ was used to measure express the fold changes between treated cells and parental cells. Average Ct value (n = 3) was used to measure the fold change. The equation used to calculate fold changes was as follows: $\Delta Ct = Ct_{sample} - Ct_{18SrRNA}$; $-\Delta\Delta Ct$ = –(unknown dCt – parental dCt); and the fold change is $2^{-\Delta\Delta Ct}$ (19).

To perform qPCR, primers were designed using the Roche webpage and the Universal Probe Library following the manufacturer's recommendationa. Primers used were as follows: Tenascin-4324(+): 5′-CCTTGCTGTAGAGGTCGTCA-3′, Tenascin-4389(−): 5′-CCAACCTCAGACACGGCTA-3′, and universal probe #14; Versican-9604(+): 5′-GCACCTGTGTGCCAGGATA-3′, Versican-9673(−): 5′-CAGGGATTAGAGTGACATTCATCA-3′, and universal probe#54; SPARC-278(+): 5′-GTGCAGAGGAAACCGAAGAG-3′, SPARC-341(−): 5′-TGTTTGCAGTGGTGGTTCTG-3′, and universal probe #77; Collagen 1-1866(+): 5′-GGGATTCCCTGGACCTAAAG-3′, Collagen 1-1928(−): 5′-GGAACACCTCGCTCTCCAG-3′, and universal probe #67; BDNF-242(+): CCGTGAGGTTTGTGTGGAC-3′, BDNF-301(−): 5′-AAAAGGATGGTCATCACTCTTCTC-3′, and universal probe #31; CCL5-101(+): 5′-CCTCATTGCTACTGCCCTCT-3′, CCL5-163(−): 5′-GGTGTGGTGTCCGAGGAATA-3′, and universal probe #16; CXCL5-407(+): 5′-CCTTTTCTAAAGAAAGTCATCCAGA-3′, CXCL5-537(−): 5′-TGGGTTCAGAGACCTCCAGA3′, and universal probe #48; and CXCL16-665(+): 5′-TGAGAGCTTACCATCGGTGTC-3′, CXCL16-737(−): 5′-TTGTTGCCTCCACACACG-3′, and universal probe #17. Three housekeeping genes, *Hydroxymethylbilane Synthase* (*HMBS*), *Hypoxanthine Guanine Phosphoribosyl Transferase 1* (*HPRT1*), and Heat-Shock 90-kDa Protein 1, β (HSPCB), were selected as suggested by Roche to confirm the consistencies of gene changes. The primers were as follows: HMBS-633(+): 5′-CGCATCTGGAGTTCAGGAGTA-3′, HMBS-722(−): 5′-CCAGGATGATGGCACTGA-3', and universal probe #18; HPRT1-136(+): 5′-TGACCTTGATTTATTTTGCATACC-3′, HPRT1-237(–): 5′-CGAGCAAGACGTTTCAGTCCT-3′, and universal probe #73; HSPCB-41(+): 5′-AGCCTACGTTGCTCACTATTACG-3′, HSPCB-136(−): 5′-GAAAGGCAAAAGTCTCCACCT-3′, and universal probe #55.

Macroarray (SuperArray) analysis

To determine extracellular matrix (ECM) gene changes in cells, 3 μg of total RNA isolated with a Qiagen RNA miniprep kit from Pt-N, Pt-C, MG_{RWV}, MG_{C4-2}, and MG_{H2O2} were used to generate cRNA with the SuperArray TrueLabeling-AMP Linear RNA Amplification kit (SuperArray Bioscience Corp.). Hybridization was performed on Oligo GEArray Microarrays (Human Extracellular Matrix and Adhesion Molecules Microarray, SuperArray). Membranes and all RNA for paired studies were processed in parallel to reduce technical variability. Chemiluminescent signals were detected on Hyperfilm enhanced chemiluminescence (Amersham Biosciences). Images were scanned into a computer for analysis at 600 dpi. Densitometry was processed by ImageJ12 and ScanAlyze13 was used for the comparative study.

Evaluation of chemokine in clinical specimens

Serum samples were collected at the Emory University School of Medicine and the National Cancer Institute (20, 21). One hundred twenty human serum specimens were collected from 40 normal, 40 local D_0 stage PCa, and 40 androgen-independent Pca (AIPC) bone metastatic patients in an NIH clinical trial. Emory specimens were collected from 10 normal and 10

[12] http://rsb.info.nih.gov/ij/
[13] http://rana.lbl.gov/

PCa patients following Institutional Review Board protocol guidelines. Sera were stored at −70°C. ELISA was performed using the Quantikine ELISA (R&D Systems) for BDNF, CCL5, CXCL5, and CXCL16. Plates were read at 450 nm and subtract readings at 570 nm to correct for optical imperfections in the plate (Molecular Devices; SpectraMax 190).

Statistical analysis

All data were log transformed to give a normal distribution, and results were confirmed by standard normal QQ plots. The measurements with no detectable tumor size (recorded as zeros) were thresholded to low values, typically half of the minimum value among the other nonzero measurements in each data set before the log-transformation. Data were subjected to a Welch two-sample test to evaluate statistical significance.

Results

Permanent morphologic changes in bone stromal cells after coculture with PCa cells under three-dimensional RWV conditions

A three-dimensional coculture model under RWV conditions was established to examine whether permanent morphologic, genetic, and behavioral changes occurred in bone stromal cells exposed to either androgen-dependent LN or androgen-independent, and bone metastatic C4-2 cells. We cocultured MG63, a human osteosarcoma cell line, or HS27A, a normal immortalized human osteoblastic cell line, with LN and C4-2 and the derivative bone stromal cells, which were designated as MG_{LN}/MG_{C4-2} and $HS27A_{LN}$/$HS27A_{C4-2}$, respectively; MG63 or HS27A cells were cultured alone as controls (MG_{RWV} and $HS27A_{RWV}$). Figure 1*A* shows that whereas there were no apparent morphologic differences between MG_{RWV} and MG_{LN}, MG_{C4-2} exhibited stable and flat spindle morphology with cells growing as parallel and light-retractile clusters. Likewise, $HS27A_{LN}$ and $HS27A_{C4-2}$ exhibited more spindled and elongated cell morphology when compared with parental HS27A and $HS27A_{RWV}$. No morphologic changes, however, were observed in the bone stromal cells after coculture with LN or C4-2 cells on plastic dishes for a similar time period (data not shown). Our observations suggest that three-dimensional RWV cell culture conditions promote permanent morphologic changes seen in MG63 and HS27A cells.

Permanent cytogenetic marker switches in MG63 cells after coculture with C4-2 cells

To determine if genetic changes may occur in concert in morphologically altered MG_{C4-2} cells, we conducted cytogenetic analyses of the MG63 cells before and after coculture with LN or C4-2 cells. C4-2 produced higher ROS than LN (22), and C4-2 rather than LN selectively induced permanent morphologic alterations of MG63. Therefore, we determined whether ROS were the common mediators of this tumor-stroma interaction. Conventional G-banding technique was used to analyze parental MG63, MG_{RWV}, MG_{LN}, and MG_{C4-2} cells. The cytogenetics of MG63 cells exposed to H_2O_2, mimicking the C4-2 cell coculture conditions, were also analyzed. Multiple chromosomal aberrations were observed in the parental osteosarcoma MG63 cells (Fig. 1*B*). After culture under three-dimensional RWV conditions, either alone or with LN or C4-2 cells, we detected consistent cytogenetic changes categorized into 3 groups (Fig. 1*B*).

Group a, parental MG63 cells, showed nonrandom characteristic marker chromosomes designated as M in box A: M1, t(1p;12q); M2, t(4q;5q); M3, del (7q); M4, t(12q;?); M5, t (11q;?), in cell lines 1 and 2, this marker is an iso (11q); M6, der (2); M7, t(8q;?;9p), a minimum of two copies of M7 were present in all spreads of these cell lines; M8, a large substelocentric chromosome with ABR (abnormally banded region); M9, t(8q;?;17q); M10, t(16q;16q); M11, a long acrocentric of unknown origin; M12, inv (7); M13, t(13q;14q); M14, del (11p); M15, a minute bisatellited chromosome. These markers are common to all

MG63 parental and derivative cell lines. Group a chromosomal markers were retained by other MG-derived cells, suggesting their lineage relationship.

Group b chromosomal markers, designated with m, were specifically associated with MG_{RWV} and MG_{LN} cells and consisted of two unique marker chromosomes, tentatively identified as m1, t(3q;12q), and m2, t(17q;?). Group c chromosomal markers, designated with *M*, were associated with the progressive changes of MG cells subsequent to cellular interaction with either LN or C4-2 cells. There were six unique clonal markers, tentatively identified as *M*1, t(2q;3q); M2, t(16q;? with ABR); *M*3, del(1q); *M*4, t(17q;ABR); M5, t(20p;?); and M6, an unidentified marker of subtelocentric morphology associated with MG_{C4-2} cells upon the examination of three clones from separate and repeated studies.

Group c markers were absent in MG63 and MG_{RWV} cell lines, and only some are present in MG_{LN} cells. MG63 cells exposed to H_2O_2 *in vitro* (Fig. 1*B*, *bottom row*) showed all six group c markers, suggesting ROS as the common mediators for the induction of stromal changes in response to tumor epithelium. The nonclonal unidentified altered chromosomes from each of these cell lines were also shown at the end of each row. Total chromosome numbers in these cell lines ranged between 42 and 143 with a peak at 134 in MG63, 122 and 64 in 2 of the MG_{RWV} clones, 112 chromosomes in MG_{LN}, a bimodal distribution of 64 and 122 chromosomes in 3 of the MG_{C4-2} clones, and 112 in H_2O_2-exposed MG63 cells. All cell lines showed aneuploidy with both structural and numerical abnormalities.

Accelerated prostate tumor growth by MG_{C4-2} cells previously exposed to PCa cells

The biological significance of MG_{C4-2} in the induction of PCa growth in athymic nude mice was investigated. Although the basal growth rate of the parental and MG63 derivatives differed slightly *in vitro*, the growth of the chimeric prostate tumors at the s.c. sites differed substantially. MG_{C4-2}/C4-2-Luc tumors grew 19-fold larger (799 ± 255 cm^3 versus 42 ± 15 cm^3) with 6-fold more serum PSA than the MG_{RWV}/C4-2-Luc chimera (1,152 ± 672 versus 192 ± 278 ng/mL; see Fig. 2*A*–*B*). Luciferase activity confirmed that the C4-2-Luc cells exhibited 19-fold higher luciferase activity in MG_{C4-2}/C4-2-Luc than MG_{RWV}/C4-2-Luc (7,659 ± 7,864 versus 401 ± 702 RLU; see Fig. 2*C*).

Prostatic stromal fibroblasts associated with PCa induced more prostate tumor growth than those associated with normal/benign prostate epithelia

Because the *bone-lineage* MG_{C4-2} was superior to MG_{RWV} and MG_{LN} in the induction of C4-2-Luc tumor growth in mice, we tested the hypothesis that stromal fibroblasts closely associated with primary tumor may be more inductive than those associated with normal/benign prostate epithelia for C4-2 tumor growth in mice. Prostate-associated stromal fibroblasts isolated from either benign/normal (Pt-N) or cancerous (Pt-C) areas of the primary prostate tissue specimens were prepared from the same patient to minimize genetic variability. Five pairs of Pt-N and Pt-C prostate fibroblasts, named Pt1-N or Pt1-C to Pt5-N or Pt5-C, were isolated. Whereas one of these five paired stromal fibroblasts, Pt1-C and Pt1-N, were compared for growth induction of C4-2-Luc tumors, all five Pt-N and Pt-C pairs were used for comparative gene expression studies. The vimentin-positive and cytokeratin- and desmin-negative prostate stromal fibroblasts from Pt1-C or Pt1-N coinoculated with C4-2-Luc cells s.c. to compare for the induction of chimeric prostate tumor growth in mice. The chimeric tumors of Pt1-C/ C4-2-Luc were 28.7-fold larger than those of the Pt1-N/C4-2, 373 ± 214 mm^3 versus 13 ± 24 mm^3, respectively. Similarly, serum PSA of the former was 233-fold more than the latter at 466 ± 358 ng/mL versus 2 ± 1.9 ng/mL, respectively (Fig. 3*A*–*B*). These results were supported by 57-fold higher Luciferase activity detected in Pt1-C/ C4-2-Luc tumor than in Pt1-N/C4-2-Luc tumor (5,154 ± 8,162 RLU versus 90 ± 149 RLU; see Fig. 3*C*).

Differential gene expression in the inductive bone cells and prostate stromal fibroblasts

Base on the dramatic growth induction differences between MG_{C4-2}/MG_{RWV} and Pt1-C/Pt1-N, we sought to compare gene expression differences among these stromal cell pairs from bone and prostate origins. We conducted an 18K microarray analysis with data analyzed by Welch two-sample test for statistical significance (23, 24). Significant gene expression changes ($P \leq 0.01$) were noted in 4,985 genes when comparing MG_{C4-2} versus MG_{RWV} and Pt1-C versus Pt1-N with 110 common genes significantly up-regulated and 54 common genes significantly down-regulated that showed a *t* test q value <10% as confirmed by J. Lee (see Supplementary Data 1–3). These included extracelluar matrix and chemokine genes. Macroarray (Supplementary Data 4–5) and qRT-PCR (data not shown) confirmed the increased expression of ECM genes such as tenascin, versican, collagen 1, and SPARC (osteonectin) in MG_{C4-2}/MG_{RWV}, and three pairs of the randomly selected prostate stromal fibroblasts. In addition, we confirmed the expression of these ECM genes in MG63 treated with H_2O_2 (see ROS data in Supplementary Data 4). Gene expressions of the chemokines and their receptors were confirmed by qRT-PCR (data not shown) and macroarray (Supplementary Data 6–7).

Confirmation of ECM and chemokine gene expression in prostate tissue and serum specimens

We focused specifically on the expression of ECM and chemokine genes by the stromal cells because these genes have been shown to regulate cell growth, survival, migration, and metastasis and can be measured reliably in prostate tissue and serum specimens. We first selected several stromal genes that showed consistent changes in microarray and macroarray, and conducted IHC analyses of the expression of these genes in PCa and adjacent stromal cells, expecting many stromal cell–expressed genes found to be deposited onto adjacent epithelium or alternatively expressed by the cancer epithelial cells. Supplementary Data 8 shows the IHC profile of tenascin, versican, and osteonectin in tissue microarray (see Supplementary Data 9 for IHC staining). Tenascin expression was elevated from 7% in normal stroma and 0% in BPH stroma to 47% in tumor-associated stroma. Versican expression was also elevated from 23% positive in normal and 9% in BPH to 44% in tumor-associated stroma. Tenascin and versican showed consistently weak staining in benign but strong staining in cancerous tissues. In contrast, osteonectin did not show significant changes between normal, benign, and cancerous prostate tissues.

Because chemokine factors are expressed in clinical specimens (25–27), we used ELISA to assess BDNF expression in serum specimens from patients who were recruited for a NCI-sponsored clinical trial and patients who underwent prostatectomy in the Department of Urology, Emory University School of Medicine. The average serum concentration of BDNF increased from normal (0 ng/mL) to D_0 (patients with localized PCa, 10.3 ± 10.1 ng/mL) and to AIPC (patients with androgen-independent, bone meta-statsis, 22.3 ± 9.5 ng/mL; Fig. 4*A*). Elevated serum BDNF was also found in serum specimens obtained from Emory Clinic (9.4 ± 5.2 ng/mL in normal and 33.1 ± 5 ng/mL in patients with localized PCa). IHC confirmed the ELISA results in which BDNF was shown to express at a low level in normal prostate epithelium but was elevated in the epithelium of both 16-week-old developing human prostate and human PCa, with the highest expression of BDNF in PCa bone metastatic specimens (data not shown). ELISA further confirmed the expression of several other chemokines in sera of normal, D_0, and AIPC patients. CCL5 increased from normal to D_0 and AIPC (0 ± 0, 4.4 ± 3.5 and 107.5 ± 44.1 ng/mL, respectively; Fig. 4*B*); CXCL5 elevated from 0.26 ± 0.54 ng/mL in normal to 2.65 ± 4.23 ng/mL in D_0 and 3.12 ± 4.32 ng/mL in AIPC patients, and CXCL16 increased from 1.2 ± 1.2 ng/mL in normal to 1.4 ± 1.0 ng/mL in D_0 and to 3.3 ± 1.5 ng/mL in AIPC patients (Fig. 4*C*–*D*).

Discussion

Interaction between stromal and epithelial cells is fundamental to the organogenesis and cytodifferentiation of the developing prostate and the maintenance of the homeostasis of the adult prostate gland (28). Upon malignant transformation, evidence suggests cancer growth, progression, and metastasis remain tightly controlled by the associated stroma in a reciprocal manner (29). Cancer-adjacent stromal cells, the “reactive stroma,” have been shown to promote the growth and progression of a large number of solid tumors including PCa (30). In this study, we showed that (*a*) both normal (HS27A) and osteosarcoma (MG63) bone stromal fibroblasts cocultured with human C4-2 PCa epithelial cells under three-dimensional RWV conditions underwent permanent morphologic changes; (*b*) the resultant stromal fibroblasts, MG63, transitioned under the inductive cue of ROS, showed permanently altered cytogenetic features, gene expression profiles, and growth-inductive properties; (*c*) transitioned stromal fibroblasts gained the ability to promote the human PCa growth when coinoculated s.c. with androgen-independent human PCa C4-2 cells in immune-compromised mice; (*d*) common stromal genes such as ECMs (tenascin and versican) and chemokines (BDNF, CCL5, CXCL5, and CXCL16) were observed to increase upon the transition of MG63 to $MG_{C4\text{-}2}$ and from Pt-N to Pt-C; and (*e*) these differentially expressed genes were confirmed in clinical specimens, where elevated expression of ECM proteins in tissue specimens and increased circulating chemokines and tissue BDNF were identified. These findings show the biological relevance of transitioned stromal fibroblasts, which are likely induced by ROS molecules, with increased expression of selective ECM proteins and chemokines promoting PCa growth in experimental models and in clinical PCa progression and lethal PCa bone metastases.

The salient features of the present study are as follows: (*a*) Coordinated changes in cytogenetic, gene expression and behavior of stromal cells can be introduced by coculture with epithelial cells under three-dimensional conditions with ROS as mediators, similar to other recent studies where laser capture microdissection of tumor-adjacent stromal cells showed consistent genetic changes (2). These results are confirmed by transgenic approaches where morphologic and gene expression profiles of the *stromal fibroblastic component* surrounding cancer epithelium can be selectively modified by prior introduced genetic changes in the epithelial cell compartment (5). (*b*) Transitioned stromal fibroblasts exhibited increased ability to promote cancer growth, consistent with the concept that reactive stroma (30) or cancer-associated stroma (31) surrounding cancer epithelium can increase the growth of cancer epithelium and help predict the survival of cancer patients. (*c*) Shared gene expression changes were found between transitioned stroma either induced experimentally under three-dimensional or isolated from clinical specimens regardless of their lineages and organs of origin (osteosarcoma versus prostate fibroblasts). Most remarkably, the shared expression of genes identified as ECM proteins and chemokines are expressed in clinical specimens, suggesting the highly conserved nature of tumor-stroma interaction. Inductive changes in stroma in response to the cancer epithelium are robust and nonrandom and may be clinically valuable for cancer diagnosis and prognosis. Our results conform to the published literature where transitioned stromal fibroblasts contributed to increased pancreatic, liver, and breast cancer growth (32–34), and increased expression of ECM proteins and chemokines in human PCa (35–40). Our results revealed increased expression of BDNF, CCL5, CXCL5, and CXCL16 in serum and/or tissue specimens of PCa patients (Fig. 4). It is likely these chemokines are produced by *both* prostatic epithelial and stromal cells because they are associated with pancreatic, prostate, colorectal, and gastric cancer epithelia (26, 40–42) and their production is related to the progression of a host of human tumors. Some of these chemokines may be intimately associated with the migration of immune reactive $CD4^+$ and $CD8^+$ cells (41) and mast cells (43). Because tumor-stroma interaction is highly conserved, our results suggest the transition of stromal

fibroblasts under the influence of cancer epithelium could be a fundamental step toward malignant progression of solid tumors. Evidence supports the reciprocal nature of tumor-stroma interaction in which the knockdown of TGFβ receptor (6) or altered p53 function in cancer-associated stroma (5) also had profound effects on PCa proliferation. Coculture (4) or coinoculation (9, 10) of prostatic or bone stromal cells with PCa epithelial cells induced permanent cytogenetic, gene expression, and behavioral changes in prostate epithelial cells. We therefore propose prostate epithelial and prostate or bone stromal cells may coevolve (Fig. 5) through (*a*) epithelial genomic, gene expression and behavioral changes as the consequence of genetic inheritance and/or altered by interaction with stromal fibroblasts; (*b*) the transitioned cancer epithelial cells induce reactive stroma responses with increased production of specific ECMs and chemokines; (*c*) reactive stroma also bear genomic, gene expression and behavioral changes that fuel the overall progression of human PCa by inducing increased growth and subsequent metastasis of PCa epithelial cells to distant organs.

Plastic dish, transwell, matrix gel, and RWV systems (4, 44, 45) have been used to study cancer-stroma interaction by coculture *in vitro*. The RWV system confirmed the genetic and gene expression changes in stromal cells induced by cancer epithelial cells. Karnoub and colleagues (46) reported the increase of CCL5 expression in tumor-associated stromal cells through direct contact with cancer epithelial cells. The RWV three-dimensional coculture model can be used to confirm factors expressed by tumor and stroma cells in experimental models and clinical specimens.

The role of ROS in PCa has been shown (47, 48). We found that H_2O_2 could play a special role mediating tumor-stroma interaction (22, 49). Cytogenetic analysis revealed identical genetic changes in MG63 cells cocultured with C4-2 cells or exposed to H_2O_2. This remarkable observation of identical cytogenetic changes in two vastly different treatment protocols suggests that the genetic alterations identified in Group c (Fig. 1*B*) could be the “hotspots” during PCa/stroma coevolution. We observed that the production of H_2O_2 by AIPC C4-2 is higher than by their androgen-dependent LN counterpart, corresponding with the ability of C4-2, but not LN, to consistently induce stromal cells to undergo permanent cytogenetic changes, coordinated gene expression profile switches, and increased induction of tumor growth in mice (22). This tumor-stroma interaction model may be highly dependent on the spatial orientation of these interactive cell types because it occurred under three-dimensional but not two-dimensional coculture conditions, consistent with our observations that genetic and coordinated gene expression changes occur in stromal fibroblasts when isolated from clinical specimens and grown as organized three-dimensional prostate tumors.

In summary, we characterized the cytogenetics, gene expression, and functions of bone and prostate stromal cells in response to three-dimensional coculture with PCa epithelial cells. The highly coordinated and conserved changes detected in both stromal and epithelial (9, 10) cells and the ability of the transitioned stromal cells to induce PCa growth and progression suggest the importance of reciprocal tumor-stroma interaction and the resultant coevolution between cancer and stroma. This concept is supported by the highly conserved gene expression profile switches observed in the prostate stromal cells isolated from clinical specimens and bone stromal cells obtained experimentally after three-dimensional coculture, which corresponded with the ECM and chemokine signatures of the clinical specimens. Further delineation of the molecular mechanisms of cellular interaction under defined spatial relationships and the roles of transitioned stromal cells and ROS in prostate carcinogenesis is warranted.

Supplementary Material

Refer to Web version on PubMed Central for supplementary material.

Acknowledgments

Grant support: NCI CA-098912 and CA-766201, NSC 96-2320-B-093-033-MY3 and NSC 96-2628-B-039-029-MY3.

References

1. Nelson WG, De Marzo AM, Isaacs WB. Prostate cancer. N Engl J Med. 2003; 349:366–381. [PubMed: 12878745]
2. Hida K, Hida Y, Amin DN, et al. Tumor-associated endothelial cells with cytogenetic abnormalities. Cancer Res. 2004; 64:8249–8255. [PubMed: 15548691]
3. Pathak S, Nemeth MA, Multani AS, Thalmann GN, von Eschenbach AC, Chung LW. Can cancer cells transform normal host cells into malignant cells? Br J Cancer. 1997; 76:1134–1138. [PubMed: 9365160]
4. Rhee HW, Zhau HE, Pathak S, et al. Permanent phenotypic and genotypic changes of prostate cancer cells cultured in a three-dimensional rotating-wall vessel. In Vitro Cell Dev Biol Anim. 2001; 37:127–140. [PubMed: 11370803]
5. Hill R, Song Y, Cardiff RD, Van Dyke T. Selective evolution of stromal mesenchyme with p53 loss in response to epithelial tumorigenesis. Cell. 2005; 123:1001–1011. [PubMed: 16360031]
6. Bhowmick NA, Chytil A, Plieth D, et al. TGF-β signaling in fibroblasts modulates the oncogenic potential of adjacent epithelia. Science. 2004; 303:848–851. [PubMed: 14764882]
7. Camps JL, Chang SM, Hsu TC, et al. Fibroblast-mediated acceleration of human epithelial tumor growth *in vivo*. Proc Natl Acad Sci U S A. 1990; 87:75–79. [PubMed: 2296606]
8. Chung LW, Matsuura J, Runner MN. Tissue interactions and prostatic growth. I. Induction of adult mouse prostatic hyperplasia by fetal urogenital sinus implants. Biol Reprod. 1984; 31:155–163. [PubMed: 6205700]
9. Hyytinen ER, Thalmann GN, Zhau HE, et al. Genetic changes associated with the acquisition of androgen-independent growth, tumorigenicity and metastatic potential in a prostate cancer model. Br J Cancer. 1997; 75:190–195. [PubMed: 9010025]
10. Thalmann GN, Anezinis PE, Chang SM, et al. Androgen-independent cancer progression and bone metastasis in the LNCaP model of human prostate cancer. Cancer Res. 1994; 54:2577–2581. [PubMed: 8168083]
11. Ricke WA, Ishii K, Ricke EA, et al. Steroid hormones stimulate human prostate cancer progression and metastasis. Int J Cancer. 2006; 118:2123–2131. [PubMed: 16331600]
12. Bond GL, Levine AJ. A single nucleotide polymorphism in the p53 pathway interacts with gender, environmental stresses and tumor genetics to influence cancer in humans. Oncogene. 2007; 26:1317–1323. [PubMed: 17322917]
13. Sung SY, Chung LW. Prostate tumor-stroma interaction: molecular mechanisms and opportunities for therapeutic targeting. Differentiation. 2002; 70:506–521. [PubMed: 12492493]
14. Nelson JB, Nabulsi AA, Vogelzang NJ, et al. Suppression of prostate cancer induced bone remodeling by the endothelin receptor A antagonist atrasentan. J Urol. 2003; 169:1143–1149. [PubMed: 12576870]
15. Storz P. Reactive oxygen species in tumor progression. Front Biosci. 2005; 10:1881–1896. [PubMed: 15769673]
16. Pathak S. Chromosome banding techniques. J Reprod Med. 1976; 17:25–28. [PubMed: 59808]
17. Gleave M, Hsieh JT, Gao CA, von Eschenbach AC, Chung LW. Acceleration of human prostate cancer growth *in vivo* by factors produced by prostate and bone fibroblasts. Cancer Res. 1991; 51:3753–3761. [PubMed: 1712249]

18. Hsieh CL, Gardner TA, Miao L, Balian G, Chung LW. Cotargeting tumor and stroma in a novel chimeric tumor model involving the growth of both human prostate cancer and bone stromal cells. Cancer Gene Ther. 2004; 11:148–155. [PubMed: 14695756]
19. Livak KJ, Schmittgen TD. Analysis of relative gene expression data using real-time quantitative PCR and the 2(−ΔΔ C(T)) Method. Methods. 2001; 25:402–408. [PubMed: 11846609]
20. Figg WD, Liu Y, Arlen P, et al. A randomized, phase II trial of ketoconazole plus alendronate versus ketoconazole alone in patients with androgen independent prostate cancer and bone metastases. J Urol. 2005; 173:790–796. [PubMed: 15711271]
21. Williams JI, Weitman S, Gonzalez CM, et al. Squalamine treatment of human tumors in nu/nu mice enhances platinum-based chemotherapies. Clin Cancer Res. 2001; 7:724–733. [PubMed: 11297269]
22. Lim SD, Sun C, Lambeth JD, et al. Increased Nox1 and hydrogen peroxide in prostate cancer. Prostate. 2005; 62:200–207. [PubMed: 15389790]
23. Chen D, Liu Z, Ma X, Hua D. Selecting genes by test statistics. Journal of biomedicine & biotechnology. 2005; 2005:132–138. [PubMed: 16046818]
24. Yang K, Li J, Gao H. The impact of sample imbalance on identifying differentially expressed genes. BMC Bioinformatics. 2006; 7 Suppl 4:S8.
25. Baer PC, Koziolek M, Fierlbeck W, Geiger H. CC-chemokine RANTES is increased in serum and urine in the early post-transplantation period of human renal allograft recipients. Kidney Blood Press Res. 2005; 28:48–54. [PubMed: 15509902]
26. Park JY, Park KH, Bang S, et al. CXCL5 overexpression is associated with late stage gastric cancer. J Cancer Res Clin Oncol. 2007; 133:835–840. [PubMed: 17479287]
27. Scala E, Pallotta S, Frezzolini A, et al. Cytokine and chemokine levels in systemic sclerosis: relationship with cutaneous and internal organ involvement. Clin Exp Immunol. 2004; 138:540–546. [PubMed: 15544634]
28. Chung LW, Cunha GR. Stromal-epithelial interactions: II. Regulation of prostatic growth by embryonic urogenital sinus mesenchyme. Prostate. 1983; 4:503–511. [PubMed: 6889194]
29. Chung LW, Gleave ME, Hsieh JT, Hong SJ, Zhau HE. Reciprocal mesenchymal-epithelial interaction affecting prostate tumour growth and hormonal responsiveness. Cancer Surv. 1991; 11:91–121. [PubMed: 1726790]
30. Tuxhorn JA, Ayala GE, Rowley DR. Reactive stroma in prostate cancer progression. J Urol. 2001; 166:2472–2483. [PubMed: 11696814]
31. Hanson JA, Gillespie JW, Grover A, et al. Gene promoter methylation in prostate tumor-associated stromal cells. J Natl Cancer Inst. 2006; 98:255–261. [PubMed: 16478744]
32. Chu GC, Kimmelman AC, Hezel AF, Depinho RA. Stromal biology of pancreatic cancer. J Cell Biochem. 2007; 101:887–907. [PubMed: 17266048]
33. Hirtenlehne K, Pec M, Kubista E, Singer CF. Extracellular matrix proteins influence phenotype and cytokine expression in human breast cancer cell lines. Eur Cytokine Netw. 2002; 13:234–240. [PubMed: 12101080]
34. Oh HS, Moharita A, Potian JG, et al. Bone marrow stroma influences transforming growth factor-β production in breast cancer cells to regulate c-myc activation of the preprotachykinin-I gene in breast cancer cells. Cancer Res. 2004; 64:6327–6336. [PubMed: 15342422]
35. Tomas D, Ulamec M, Hudolin T, Bulimbasic S, Belicza M, Kruslin B. Myofibroblastic stromal reaction and expression of tenascin-C and laminin in prostate adenocarcinoma. Prostate Cancer Prostatic Dis. 2006; 9:414–419. [PubMed: 16652121]
36. Ricciardelli C, Mayne K, Sykes PJ, et al. Elevated levels of versican but not decorin predict disease progression in early-stage prostate cancer. Clin Cancer Res. 1998; 4:963–971. [PubMed: 9563891]
37. Begley LA, Kasina S, Mehra R, et al. CXCL5 promotes prostate cancer progression. Neoplasia. 2008; 10:244–254. [PubMed: 18320069]
38. Bronzetti E, Artico M, Forte F, et al. A possible role of BDNF in prostate cancer detection. Oncol Rep. 2008; 19:969–974. [PubMed: 18357383]
39. Lu Y, Wang J, Xu Y, et al. CXCL16 functions as a novel chemotactic factor for prostate cancer cells *in vitro*. Mol Cancer Res. 2008; 6:546–554. [PubMed: 18344492]

40. Vaday GG, Peehl DM, Kadam PA, Lawrence DM. Expression of CCL5 (RANTES) and CCR5 in prostate cancer. Prostate. 2006; 66:124–134. [PubMed: 16161154]
41. Hojo S, Koizumi K, Tsuneyama K, et al. High-level expression of chemokine CXCL16 by tumor cells correlates with a good prognosis and increased tumor-infiltrating lymphocytes in colorectal cancer. Cancer Res. 2007; 67:4725–4731. [PubMed: 17510400]
42. Schneider MB, Standop J, Ulrich A, et al. Expression of nerve growth factors in pancreatic neural tissue and pancreatic cancer. J Histochem Cytochem. 2001; 49:1205–1210. [PubMed: 11561004]
43. Guettier C, Validire P, Emilie D, et al. Follicular dendritic cell tumor of the mediastinum: expression of fractalkine and SDF-1a as mast cell chemoattractants. Virchows Arch. 2006; 448:218–222. [PubMed: 16408220]
44. Kunz-Schughart LA, Freyer JP, Hofstaedter F, Ebner R. The use of 3-D cultures for high-throughput screening: the multicellular spheroid model. J Biomol Screen. 2004; 9:273–285. [PubMed: 15191644]
45. Zhang S. Designer self-assembling Peptide nanofiber scaffolds for study of 3-d cell biology and beyond. Adv Cancer Res. 2008; 99:335–362. [PubMed: 18037409]
46. Karnoub AE, Dash AB, Vo AP, et al. Mesenchymal stem cells within tumour stroma promote breast cancer metastasis. Nature. 2007; 449:557–563. [PubMed: 17914389]
47. Frohlich DA, McCabe MT, Arnold RS, Day ML. The role of Nrf2 in increased reactive oxygen species and DNA damage in prostate tumorigenesis. Oncogene. 2008; 27:4353–4362. [PubMed: 18372916]
48. Kumar B, Koul S, Khandrika L, Meacham RB, Koul HK. Oxidative stress is inherent in prostate cancer cells and is required for aggressive phenotype. Cancer Res. 2008; 68:1777–1785. [PubMed: 18339858]
49. Shigemura K, Sung SY, Kubo H, et al. Reactive oxygen species mediate androgen receptor- and serum starvation-elicited downstream signaling of ADAM9 expression in human prostate cancer cells. Prostate. 2007; 67:722–731. [PubMed: 17342749]

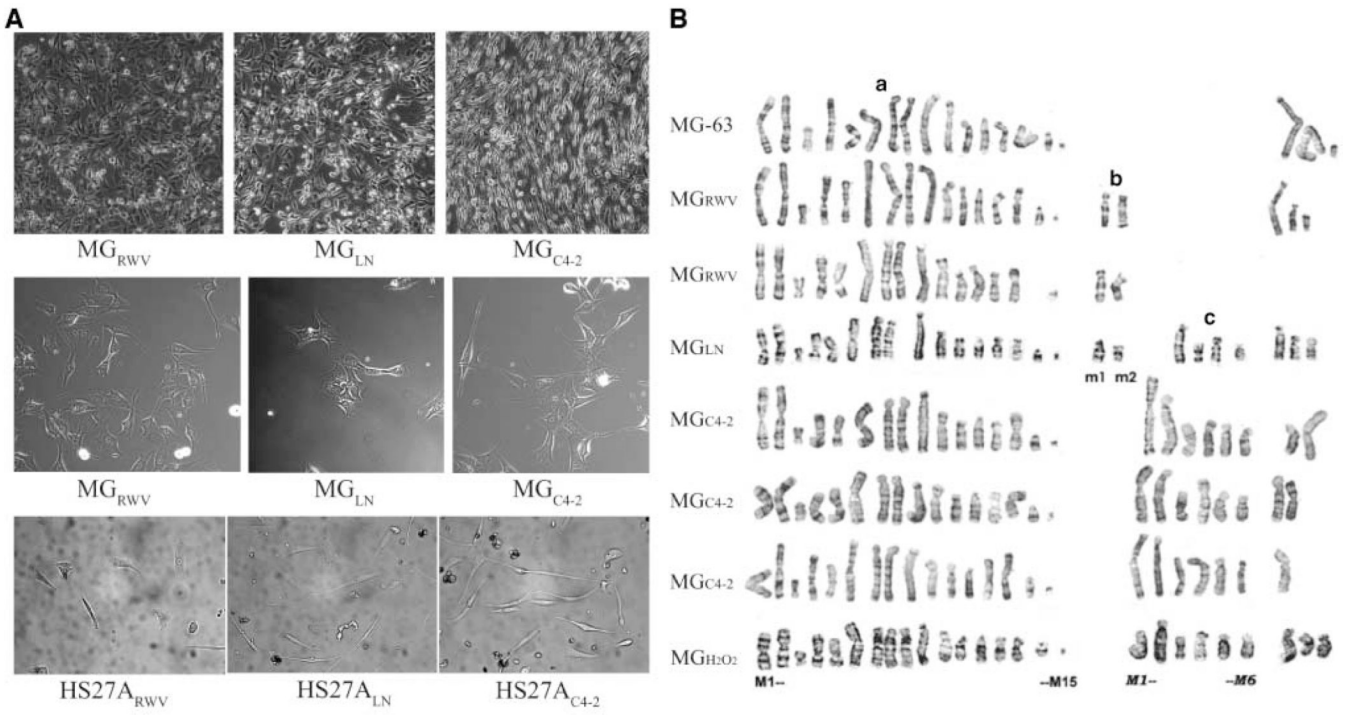

Figure 1.

A, morphology of osteosarcoma bone cell line MG_{C4-2} differed from MG_{RWV} and MG_{LN} at 90%confluence (*top*). MG_{C4-2} showed parallel, light-retractile, and flatter spindle cell alignment. No apparent cell morphologic difference was detected at a lower cell density (*middle*). Similar morphologic changes were also observed in a HS27A derivative, $HS27A_{C4-2}$, after cellular interaction with C4-2 cells, compared with $HS27A_{LN}$ and $HS27A_{RWV}$ (*bottom*). *B*, giemsa-banded marker chromosomes of parental MG63, MG-derivatives (MG_{RWV}, MG_{LN}, and MG_{C4-2}), and MG63 exposed to H_2O_2 (MG_{H2O2}). *Group a*, (*M1-M15*) shared marker chromosomes between these cell lines. *Group b*, markers (*m1* and *m2*) shared only by MG_{RWV} and MG_{LN} cell lines. *Group c*, six additional marker chromosomes (*m1–m6*) shared by MG_{C4-2} and MG63 cells exposed to H_2O_2. MG_{LN} cells have only some of the group *c* markers. Nonclonal and unidentified altered chromosomes from each cell line are arranged on the far right (see text for group *a*, *b*, and *c* marker chromosomes).

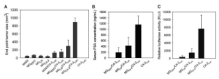

Figure 2.

MG_{C4-2} with altered morphology and cytogenetics was more inductive than MG_{LN} and MG_{RWV} in chimeric prostate tumor growth in mice. *A*, chimeric C4-2-Luc tumors produced by coinjecting with MG_{C4-2} grew significantly faster than those from MG_{RWV}, MG_{LN}, or in the absence of MG cells (*columns*, mean of tumor volume of five independent measurements; *bars*, SE). C4-2-Luc alone failed to form tumors in mice (*A*). These data agree with serum PSA (*B*) and chimeric tumor epithelial cell-associated luciferase activity (*C*).

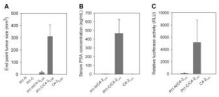

Figure 3.
Increased chimeric tumor growth in mouse s.c. space by coinjection of Pt1-C or Pt1-N with C4-2-Luc cells. A, representative chimeric tumor growth in athymic mice after coinjecting Pt1-C or Pt1-N cells and C4-2-Luc cells s.c. Larger chimeric tumors were detected with Pt1-C/C4-2 than Pt1-N/C4-2. Tumor size distributions were obtained at the end of the study. Pt1-C was more inductive than Pt1-N for the growth of androgen-independent and bone metastatic C4-2 cells ($P = 0.001$), confirmed by mouse serum PSA ($P = 0.002$; *B*) and tumor-associated luciferase activity ($P = 0.021$; *C*).

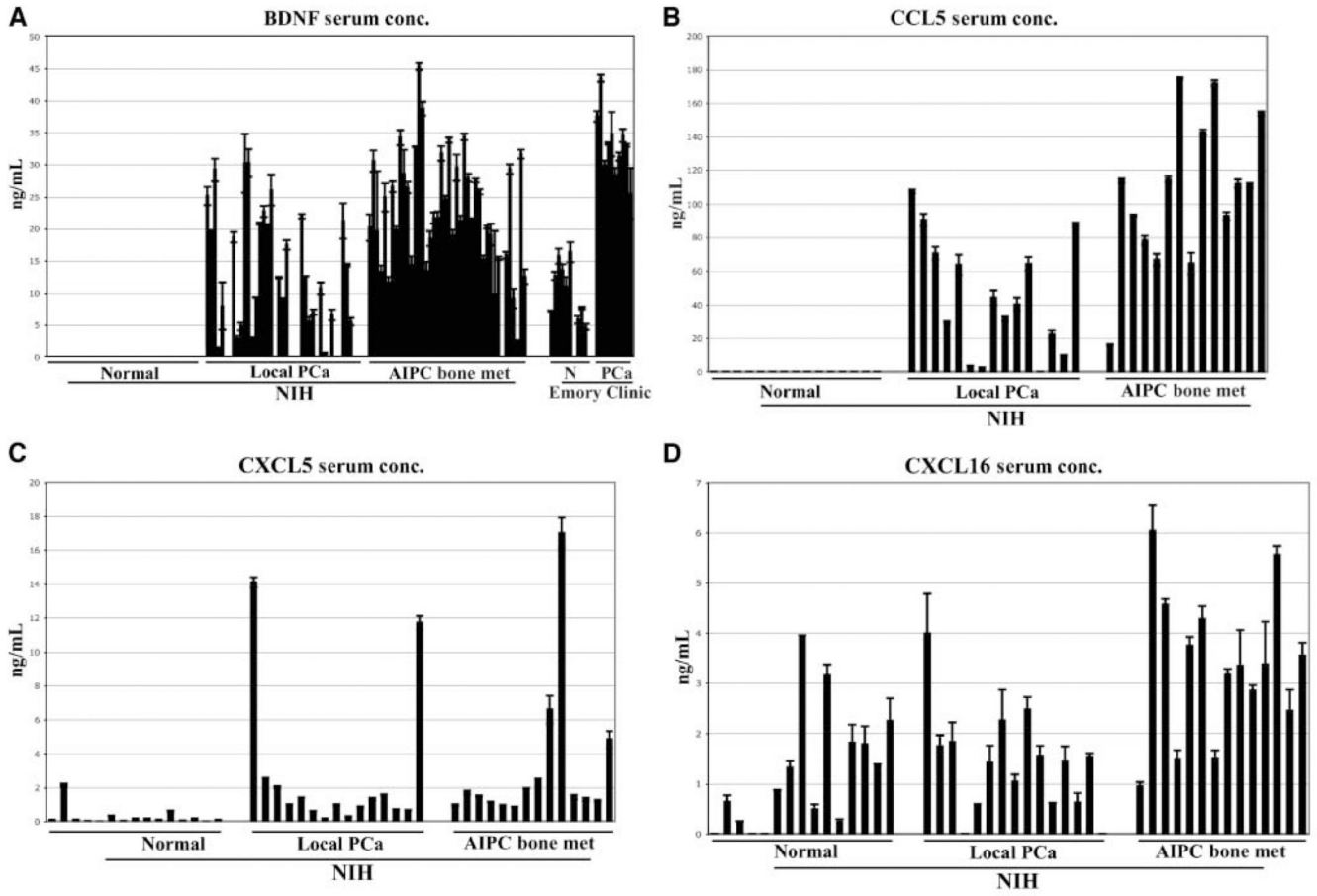

Figure 4.

Serum concentrations (*conc*.) of circulating chemokines, BDNF, CCL5, CXCL5, and CXCL16, in the sera of PCa patients and BDNF in human PCa bone metastatic specimens in patients with localized (*Local PCa*) and androgen-independent bone metastatic PCa (*AIPC bone met*). Control sera from age-matched normal healthy controls. *A*, BDNF quantified by ELISA in both NIH and Emory specimens. Serum specimens from NIH were quantified by ELISA for CCL5 (*B*), CXCL5 (*C*), and CXCL16 (*D*).

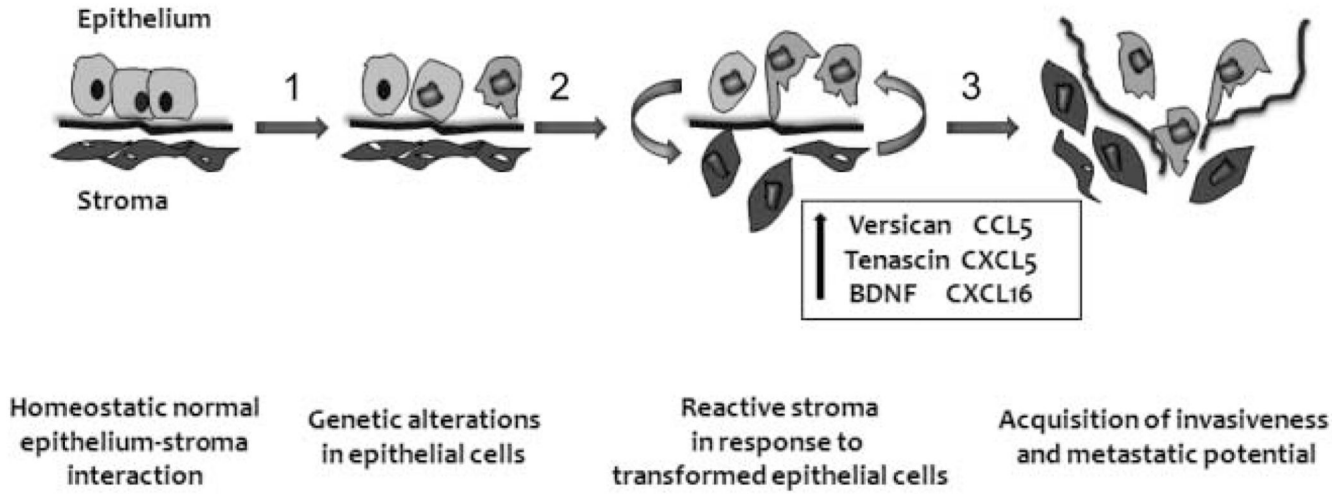

Figure 5.

Coevolution of PCa and bone stromal cells upon cellular interaction under three-dimensional coculture conditions. *1*, normal epithelial cells break away from homeostatic constraint and undergo genetic changes; *2*, stromal cells reactivated to altered epithelium by expressing increased ECMs, proinvasive cytokines, and chemokines; *3*, reactive stroma promote PCa cells through paracrine signaling to acquire increased growth and metastatic potential.